the plant journal

SEB Society for Experimental Biology

The Plant Journal (2012) **72**, 331–344 doi: 10.1111/j.1365-313X.2012.05084.x

Systematic silencing of benzylisoquinoline alkaloid biosynthetic genes reveals the major route to papaverine in opium poppy

Isabel Desgagné-Penix and Peter J. Facchini*

Department of Biological Sciences, University of Calgary, Calgary, AB T2N 1N4, Canada

Received 26 April 2012; revised 17 June 2012; accepted 19 June 2012; published online 9 August 2012.
*For correspondence (e-mail pfacchin@ucalgary.ca).

SUMMARY

Papaverine, a major benzylisoquinoline alkaloid in opium poppy (*Papaver somniferum*), is used as a vasodilator and antispasmodic. Conversion of the initial intermediate (*S*)-norcoclaurine to papaverine involves 3′-hydroxylation, four *O*-methylations and dehydrogenation. However, our understanding of papaverine biosynthesis remains controversial more than a century after an initial scheme was proposed. *In vitro* assays and *in vivo* labeling studies have been insufficient to establish the sequence of conversions, the potential role of the intermediate (*S*)-reticuline, and the enzymes involved. We used virus-induced gene silencing in opium poppy to individually suppress the expression of six genes with putative roles in papaverine biosynthesis. Suppression of the gene encoding coclaurine *N*-methyltransferase dramatically increased papaverine levels at the expense of *N*-methylated alkaloids, indicating that the main biosynthetic route to papaverine proceeds via *N*-desmethylated compounds rather than through (*S*)-reticuline. Suppression of genes encoding (*S*)-3′-hydroxy-*N*-methylcoclaurine 4-*O*-methyltransferase and norreticuline 7-*O*-methyltransferase, which accept certain *N*-desmethylated alkaloids, reduced papaverine content. In contrast, suppression of genes encoding *N*-methylcoclaurine 3′-hydroxylase or reticuline 7-*O*-methyltransferase, which are specific for *N*-methylated alkaloids, did not affect papaverine levels. Suppression of norcoclaurine 6-*O*-methyltransferase transcript levels significantly suppressed total alkaloid accumulation, implicating (*S*)-coclaurine as a key branch-point intermediate. The differential detection of *N*-desmethylated compounds in response to suppression of specific genes highlights the primary route to papaverine.

Keywords: *Papaver somniferum*, opium poppy, benzylisoquinoline alkaloids, functional genomics, metabolic engineering, secondary metabolism, virus-induced gene silencing.

INTRODUCTION

Opium poppy (*Papaver somniferum*) produces a variety of structurally diverse benzylisoquinoline alkaloids (BIAs), many of which possess potent pharmacological activities, including the narcotic analgesics codeine and morphine, the potential anti-cancer drug noscapine, the antimicrobial agent sanguinarine and the vasodilator papaverine (Figure 1). Papaverine has also been used as an antispasmodic drug for treatment of intestinal and urinary tract spasms, bronchial asthma, renal and biliary colic, pulmonary arterial embolism, migraine headaches and schizophrenia (Brisman *et al.*, 2006; Damen *et al.*, 2006; Mindea *et al.*, 2006; Menniti *et al.*, 2007; McGeoch and Oldroyd, 2008; Srivastava *et al.*, 2011), and as a smooth muscle relaxant in microsurgery and occasionally to treat erectile disorders (Bella and Brock, 2004; Desvaux, 2005; Barry, 2007; Priebe, 2007). Although the pharmacological mechanism is unclear, papaverine is known to increase cAMP levels by inhibiting phosphodiesterases (Boswell-Smith *et al.*, 2006; Menniti *et al.*, 2007). Cultivated opium poppy plants remain the sole commercial source for codeine, morphine and noscapine, due primarily to the occurrence of chiral centers in many BIA backbone structures. However, methods for the industrial synthesis of papaverine, which lacks a chiral center, have been established. Indeed, chemical synthesis is essential because the demand for papaverine currently exceeds its potential supply through the licit cultivation of opium poppy.

Papaverine was the first opium alkaloid for which a hypothetical biosynthetic pathway was proposed. The original scheme suggested that the BIA backbone was derived

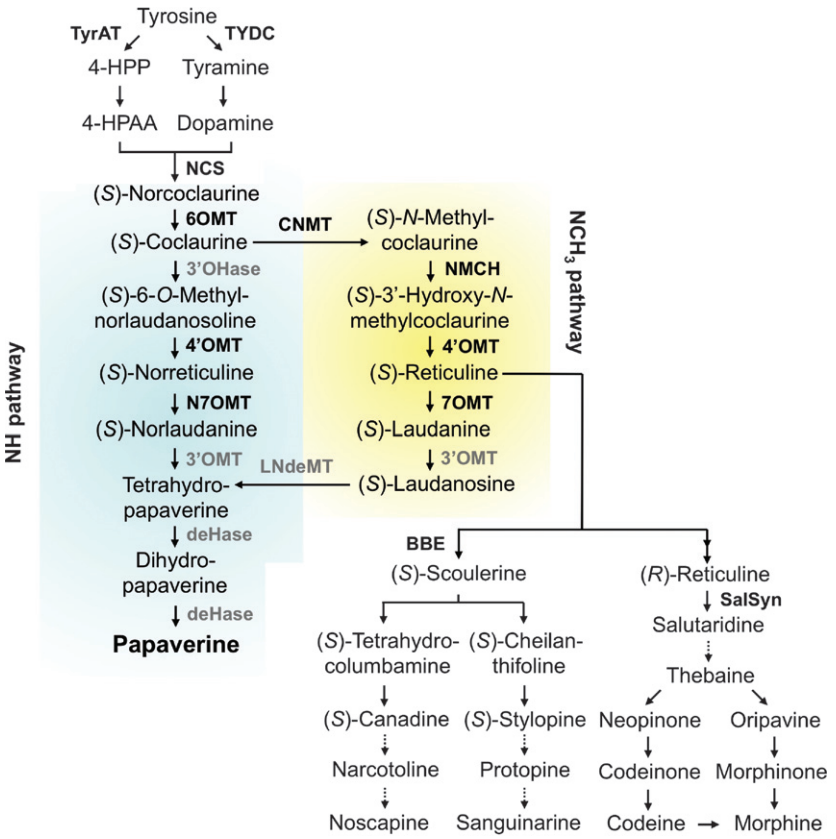

Figure 1. Biosynthetic pathways leading to the major alkaloids in opium poppy.
Enzymes for which cognate cDNAs have been isolated from opium poppy are shown in black, whereas those in gray have not been characterized. Dotted arrows indicate more than one catalytic conversion. Blue and yellow highlighting indicates *N*-desmethylated (the NH pathway) and *N*-methylated (the NCH_3 pathway) compounds, respectively. Abbreviations: TyrAT, tyrosine aminotransferase; TYDC, tyrosine decarboxylase; NCS, norcoclaurine synthase; 6OMT, (*S*)-norcoclaurine 6-*O*-methyltransferase; CNMT, (*S*)-coclaurine *N*-methyltransferase; NMCH, (*S*)-*N*-methylcoclaurine 3′-hydroxylase; 3′OHase, 3′-hydroxylase; 4′OMT, (*S*)-3′-hydroxy-*N*-methylcoclaurine 4′-*O*-methyltransferase; N7OMT, norreticuline 7-*O*-methyltransferase; 7OMT, reticuline 7-*O*-methyltransferase; 3′OMT, 3′-*O*-methyltransferase; deHase, dehydrogenase; LNdeMT, laudanosine *N*-demethylase; BBE, berberine bridge enzyme; SalSyn, salutaridine synthase.

through condensation of dopamine and 3,4-dihydroxyphenylacetaldehyde to yield the tetrahydroxylated compound (*S*)-norlaudanosoline (Winterstein and Trier, 1910). More recently, the central precursor to all BIAs was identified as the trihydroxylated intermediate (*S*)-norcoclaurine (Stadler *et al.*, 1987; Frenzel and Zenk, 1990; Stadler and Zenk, 1990), which is formed via condensation of the tyrosine derivatives dopamine and 4-hydroxyphenylacetaldehyde by norcoclaurine synthase (NCS) (Samanani *et al.*, 2004; Lee and Facchini, 2010) (Figures 1 and S1). Nevertheless, labeling patterns resulting from feeding of [^{13}C]-tyrosine to *Coptis japonica* cell cultures showed the correct position-specific incorporation of norlaudanosoline and other potential biosynthetic precursors into papaverine due the relatively broad substrate range of several early biosynthetic enzymes. For example, norcoclaurine 6-*O*-methylcoclaurine (6OMT) was shown to prefer (*S*)-norcoclaurine as a substrate, but also efficiently accepted (*S*)-norlaudanosoline (Sato *et al.*, 1994). Subsequent 6-*O*-methylation, *N*-methylation, 3′-hydroxylation and 4′-*O*-methylation convert (*S*)-norcoclaurine to (*S*)-reticuline, which is a branch-point intermediate in the formation of most BIA structural sub-groups, including morphinan (e.g. morphine), phthalideisoquinoline (e.g. noscapine) and benzophenanthridine (e.g. sanguinarine) alkaloids.

Our understanding of papaverine biosynthesis remains controversial more than a century after the pathway was first suggested. Two metabolic routes from (*S*)-norcoclaurine have been proposed. One consists entirely of *N*-desmethylated intermediates (the NH pathway), whereas the other proceeds through several *N*-methylated intermediates and involves (*S*)-reticuline (the NCH_3 pathway) (Figures 1 and S1). The validity of the NH pathway is supported by early feeding experiments with labeled precursors combined with controlled degradation of labeled papaverine, which showed incorporation of tyramine, dopamine and 4-hydroxyphenylacetaldehyde (Battersby and Binks, 1960; Battersby and Harper, 1962; Battersby, 1963; Battersby *et al.*, 1964, 1965; Brochmann-Hanssen *et al.*, 1971, 1975, 1980). The BIAs norlaudanosoline, norreticuline, norlaudanine and tetrahydropapaverine were incorporated into papaverine, although reticuline was not (Uprety *et al.*, 1975). The recent isolation and *in vitro* functional characterization of norreticuline-7-*O*-methyltransferase (N7OMT), which catalyzes the 7-*O*-methylation of norreticuline to norlaudanine, from papaverine-producing opium poppy seedlings provided biochemical support for the NH pathway (Pienkny *et al.*, 2009). Accordingly, papaverine biosynthesis has been proposed to involve 3′-hydroxylation of the 6-*O*-methylated BIA (*S*)-coclaurine, forming (*S*)-6-*O*-methylnorlaudanosoline, followed by three *O*-methylations at C7, C3′ and C4′ to yield tetrahydropapaverine, which is subsequently dehydrogenated to dihydropapaverine and papaverine (Figures 1

and S1). Although such conversions could proceed via several permutations, some restrictions have been proposed. For example, feeding experiments suggested that 6-*O*-methylation occurs before 7-*O*-methylation, and that the dehydrogenation of tetrahydropapaverine occurs only subsequent to all four *O*-methylation reactions (Brochmann-Hanssen *et al.*, 1971, 1975). Intuitively, 3′-hydroxylation must occur prior to 3′-methylation. For clarity, pathways are depicted according to the proposed biosynthesis of (*S*)-reticuline (Pienkny *et al.*, 2009) (Figures 1 and S1).

In contrast to the proposed involvement of *N*-desmethylated intermediates, isotope dilution analysis suggested that norlaudanosoline and norreticuline are not naturally occurring intermediates in BIA metabolism (Stadler and Zenk, 1990). More recently, the formation of papaverine via (*S*)-reticuline was proposed based on studies using heavy isotope-labeled precursors (Han *et al.*, 2010). Labeled (*S*)-coclaurine and (*S*)-reticuline were incorporated into papaverine and thebaine in opium poppy seedlings. In the proposed NCH_3 pathway, (*S*)-reticuline is converted to (*S*)-laudanine by reticuline 7-*O*-methyltransferase (7OMT) (Ounaroon *et al.*, 2003) and subsequently 3′-*O*-methylated to form (*S*)-laudanosine (Han *et al.*, 2010). Finally, the *N*-demethylation of laudanosine yields tetrahydropapaverine, which is dehydrogenated to papaverine (Figures 1 and S1). Although both putative pathways involve 3′-hydroxylation, C6, C7, C3′ and C4′ *O*-methylation and ultimate dehydrogenation, the NCH_3 pathway also includes *N*-methylation and subsequent *N*-demethylation steps.

In this study, we systematically suppress six genes encoding known BIA biosynthetic enzymes potentially involved in the two proposed biosynthetic schemes leading to papaverine using virus-induced gene silencing (VIGS) in opium poppy plants. The NH pathway was identified as the main metabolic route to papaverine in the investigated variety of opium poppy. Our results also show that the early BIA pathway involves a matrix of functional group substitutions as opposed to the generally depicted linear sequence of conversions yielding (*S*)-reticuline as a central branch-point intermediate.

RESULTS

VIGS reduces BIA biosynthetic gene transcript levels

Virus-induced gene silencing (VIGS) in opium poppy was used to functionally characterize six genes potentially involved in papaverine biosynthesis. The selected enzymes operate at, or near, putative branch points in the two proposed metabolic routes (Figures 1 and S1). Gene-specific fragments of *6OMT*, coclaurine *N*-methyltransferase (*CNMT*), *N*-methylcoclaurine 3′-hydroxylase (*NMCH*), 3′-hydroxy-*N*-methylcoclaurine *O*-methyltransferase 2 (*4′OMT2*), *N7OMT* and *7OMT* were inserted independently into pTRV2 (Figure S2). Initially, RT-PCR was performed to identify plants infected with tobacco rattle virus (TRV) by detection of viral coat protein transcripts (Figure S3). Opium poppy glyceraldehyde 3-phosphate dehydrogenase was used as an endogenous control. Nine TRV-positive plants were selected for each of the gene-specific constructs and the empty vector control.

To confirm the suppression of targeted transcripts, real-time quantitative PCR was performed using primer pairs that annealed to nucleotide sequences outside the gene fragments used to construct pTRV2 vectors (Table S1). Efficient suppression of each target gene was detected (Figure 2), but closely related genes were generally not affected (Figure S4). For example, plants infiltrated with *Agrobacterium tumefaciens* harboring pTRV2-4′OMT2 displayed significantly reduced levels of *4′OMT2* transcripts, but showed no effect on the abundance of *4′OMT1* transcripts compared

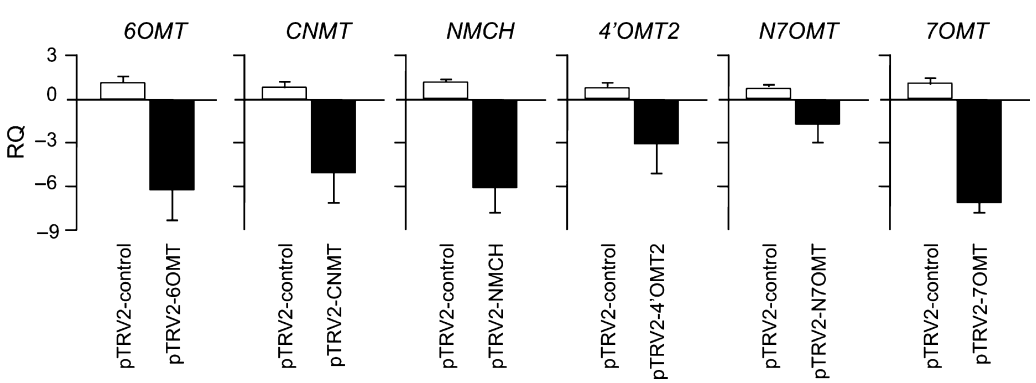

Figure 2. Real-time quantitative PCR analysis of target gene transcript levels in stems from opium poppy plants subjected to VIGS.
Total RNA from stems was isolated, reverse transcribed and used as a template for real-time quantitative PCR with SYBR Green detection. Values are means ± standard deviation of three technical replicates for each of three biological replicates from nine individual plants. Normalization was performed using ubiquitin as the reference transcript. Relative quantity (RQ) was calculated using the equation: $RQ = 2^{-\Delta\Delta C_t}$, with the pTRV2 control serving as the calibrator. White bars and black bars represent the pTRV2 control and corresponding gene-specific pTRV2 constructs, respectively. All mean values were statistically significantly different relative to the corresponding pTRV2 control using Student's *t*-test at $P < 0.05$.

with control plants. Similarly, silencing *6OMT* did not significantly affect the relative abundance of *4′OMT2* transcripts. However, one exception involved suppression of *CNMT* expression, which was consistently associated with a reduction in the relative abundance of *NMCH*, *4′OMT2* and salutaridine synthase transcripts (Figure S4).

Suppression of biosynthetic gene expression alters BIA content

Alkaloid profiles in the latex of opium poppy infiltrated with *A. tumefaciens* harboring the various pTRV2 constructs were initially screened by TLC (Figure S5) and subsequently determined using HPLC (Figure 3). The mean BIA composition of control plants was 38% morphine, 14% codeine, 16% thebaine, 2% oripavine, 12% papaverine, 3% reticuline and 15% noscapine (Figures 3 and 4). Plants with suppressed *6OMT* transcript levels displayed a total alkaloid content that was 73% lower than controls (Figures 3 and 4). However, the relative abundance of morphine increased to 55% of the total alkaloid content. Plants exhibiting reduced *CNMT* transcript levels showed a significant fourfold increase in the relative abundance of papaverine, and a reduction in the accumulation of thebaine and noscapine. Silencing of *NMCH* was associated with a 22% reduction in total alkaloid accumulation, with a notable decrease in the levels of thebaine and codeine compared with controls. In contrast, absolute levels of morphine and papaverine were not affected, resulting in an increased abundance of each compound relative to other alkaloids. Silencing of *4′OMT2* also resulted in a significant 43% reduction in total alkaloid content due to a decrease in accumulation of most major alkaloids, including noscapine, papaverine, thebaine, codeine, and, to a lesser extent, morphine. Suppression of *N7OMT* transcript levels caused a significant decrease in papaverine accumulation, but had no detectable effect on the relative abundance of other BIAs and did not alter total alkaloid levels compared with controls (Figures 3 and 4). In contrast to the other five target genes, the suppression of *7OMT* expression increased total BIA content, but did not significantly alter the relative abundance of major alkaloids (Figure 4). The independent suppression of three genes (i.e. *CNMT*, *NMCH* and *4′OMT2*) each caused a reduction in the relative abundance of thebaine, oripavine and/or codeine, but did not affect morphine levels.

Correlation between relative transcript abundance and papaverine content

Comparison of target gene transcript levels and papaverine content in individual opium poppy plants infiltrated with *A. tumefaciens* harboring control and gene-specific pTRV2 constructs revealed three positive, one negative and two null correlations (Figure 5). *6OMT*, *4′OMT2* and *N7OMT* transcript levels correlated positively with papaverine accumulation. All plants displaying a reduction in the relative abundance of each transcript also exhibited significantly lower papaverine content compared with controls. In contrast, *CNMT* transcript levels showed a strong negative correlation with papaverine accumulation. Plants with sup-

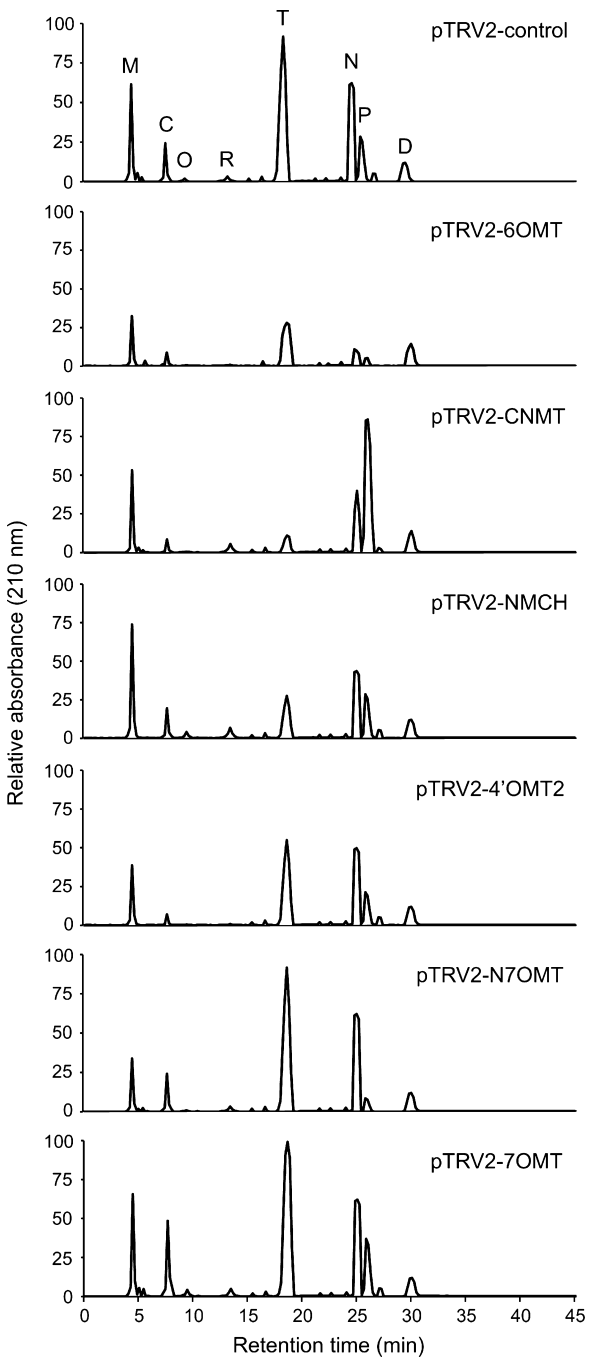

Figure 3. HPLC analysis of latex extracts from opium poppy plants subjected to VIGS using the indicated constructs.
Latex quantity was normalized based on protein concentration. Absorbance was measured at 210 nm. Dextromethorphan was used as an internal standard for extraction efficiency and relative quantification. Peaks corresponding to the retention times of authentic standards are indicated. Abbreviations: M, morphine; C, codeine; O, oripavine; R, reticuline; T, thebaine; N, noscapine; P, papaverine; D, dextromethorphan.

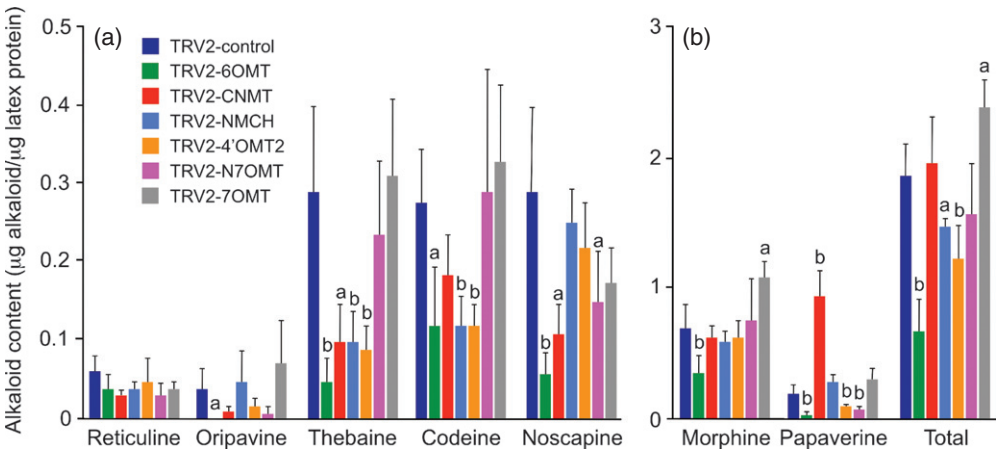

Figure 4. Abundance of major BIAs in latex extracts of opium poppy plants subjected to VIGS using the indicated constructs.
Values are means ± standard deviation of specific and total alkaloid contents in latex extracts from nine independent plants for each target gene. Letters above the bars indicate mean values that are statistically different relative to the corresponding pTRV2 control using Student's *t* test: $^{a}P < 0.05$; $^{b}P < 0.01$.
(a) Relative abundance of reticuline, oripavine, thebaine, codeine and noscapine.
(b) Relative abundance of morphine, papaverine and total alkaloid content.

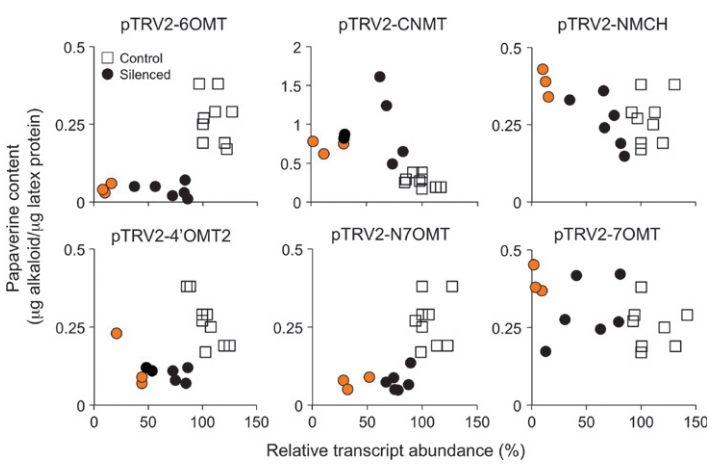

Figure 5. Correlation between the relative abundance of target gene transcripts and the level of papaverine in opium poppy plants subjected to VIGS using the indicated pTRV2 constructs (circles) or empty vector (squares).
Orange circles represent the plants selected for LC-MS analysis.

pressed *CNMT* transcript levels had substantially higher papaverine content compared with controls. Suppression of *NMCH* or *7OMT* did not affect papaverine accumulation.

LC-MS analysis of VIGS plants

The three plants that showed the greatest reduction in target transcript abundance were selected from populations of plants infiltrated with *A. tumefaciens* harboring corresponding gene-specific pTRV2 constructs (Figure 5). Three control plants were also randomly selected. Latex extracts were subjected to LC-MS to determine the relative abundance of compounds not detected using HPLC (Table S2).

The effects of silencing target genes on BIA content were confirmed using LC-MS (Table S2). Morphine, codeine, thebaine, papaverine and noscapine accounted for approximately 77% of the total characterized BIA content in control plant latex. LC-MS allowed detection of additional low-abundance alkaloids for which authentic standards were not available (Figure 6 and Table S2). These included compounds that participate in the morphinan (e.g. dehydroreticuline and salutaridine) and phthalideisoquinoline (e.g. narcotoline and *N,N*-dimethylnarcotine) branch pathways, and the minor alkaloids protoberberine and protopine. The only detected pathway intermediate in the established (*S*)-reticuline pathway was *N*-methylcoclaurine (Figure 1). The intermediates norcoclaurine, coclaurine and 3′-hydroxy-*N*-methylcoclaurine were not detected. However, a number of differentially substituted BIAs (4′-*O*-methylcoclaurine, *N,N*-dimethylcoclaurine, *N*-methyl-4′-*O*-methylcoclaurine, norreticuline, pacodine, palaudine, norlaudanine, codamine, laudanine, tetrahydropapaverine and laudanosine) were detected (Figures 6 and S6 and Table S2).

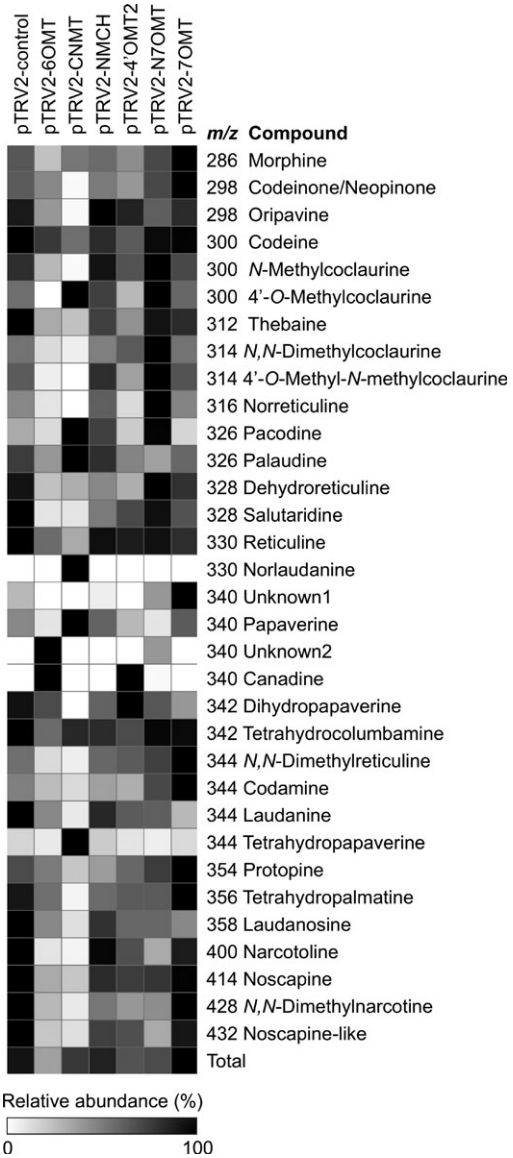

Figure 6. Heat map showing relative BIA levels in latex extracts of opium poppy plants subjected to VIGS using the indicated constructs.
Relative abundance was determined by LC-MS, and is normalized to the sample with the highest level of each compound (i.e. abundance can be compared across rows, but not down columns). Corresponding values are provided in Table S2.

A heat map showing relative alkaloid abundance in the latex of plants with individually suppressed target genes is shown in Figure 6. Most alkaloid levels were substantially lower in opium poppy plants with reduced *6OMT* transcript levels compared with controls (Figure 6 and Table S2). However, two compounds, canadine and an unknown compound (unknown2), accumulated in *6OMT*-suppressed plants to levels higher than in controls. Canadine levels also increased in *4′OMT2*-silenced plants. The increased papaverine content of *CNMT*-silenced plants was accompanied by accumulation of the *N*-desmethylated compounds 4′-*O*-methylcoclaurine, norlaudanine and tetrahydropapaverine and the dehydrogenated derivatives pacodine (7-*O*-demethylpapaverine) and palaudine. Although most of these compounds were detected at low levels in control plants, norlaudanine was only detected in *CNMT*-suppressed plants. The levels of several *N*-methylated compounds, including *N*-methylcoclaurine, *N,N*-dimethylcoclaurine, 4′-*O*-methyl-*N*-methylcoclaurine, reticuline, *N,N*-dimethylreticuline, codamine, laudanine, laudanosine and salutaridine, and four phathelideisoquinoline alkaloids (i.e. narcotoline, noscapine, *N,N*-dimethylnarcotine and another noscapine-like compound) were also reduced in *CNMT*-suppressed plants.

In *NMCH*-suppressed plants, the level of the NMCH substrate *N*-methylcoclaurine increased together with those of 4′-*O*-methyl-*N*-methylcoclaurine (Figures 6 and 7 and Table S2). *4′OMT2*-silenced plants showed a reduction of 4′-*O*-methylcoclaurine, *N*-methyl-4′-*O*-methylcoclaurine, norreticuline, dehydroreticuline, reticuline, papaverine, codamine, laudanine, laudanosine, morphinan alkaloids (i.e. thebaine, codeinone/neopinone and codeine) and phathelideisoquinoline alkaloids (i.e. narcotoline, noscapine, *N,N*-dimethylnarcotine and a noscapine-like compound). *N7OMT*-suppressed plants showed reduced levels of papaverine, tetrahydropapaverine, palaudine, pacodine and reticuline. An accumulation of the N7OMT substrate norreticuline was associated with increased relative abundance of putative pathway intermediates and *N*-methylated derivatives (i.e. 4′-*O*-methylcoclaurine, *N*-methyl-4′-*O*-methylcoclaurine, *N*-methylcoclaurine, *N,N*-dimethylcoclaurine and dehydroreticuline) (Figures 6 and 7 and Table S2). Suppression of *7OMT* expression did not affect the content of *N*-desmethylated compounds including papaverine. However, the relative abundance of the *N*-methylated alkaloids laudanine and laudanosine was reduced. Several other compounds, including morphine and noscapine, accumulated at higher levels compared with controls.

DISCUSSION

Biochemical roles for several genes involved in the formation of BIA precursors (Lee and Facchini, 2011), (*S*)-norcoclaurine (Lee and Facchini, 2010) and morphinan alkaloid branch pathway intermediates (Hagel and Facchini, 2010; Wijekoon and Facchini, 2012) have been established using VIGS. Recently, the use of VIGS to decipher plant metabolic networks has also been reported for other pathways, including monoterpenoid indole alkaloid biosynthesis (Liscombe and O'Connor, 2011) and starch degradation (George *et al.*, 2012). Here we use the systematic suppression of known and potentially relevant biosynthetic genes to reveal the major metabolic route to papaverine. Despite the straightforward functional group modifications involved in conversion of (*S*)-norcoclaurine

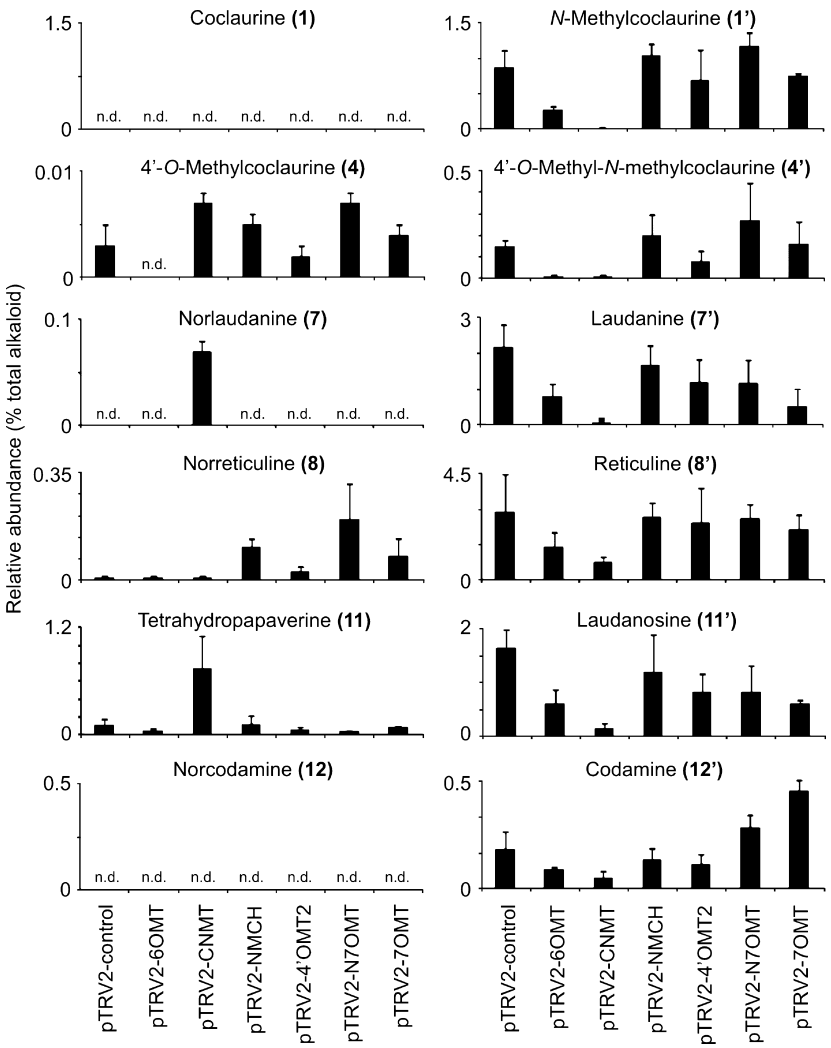

Figure 7. Relative abundance of BIAs in latex extracts of opium poppy subjected to VIGS using the indicated constructs. Relative abundance was determined by LC-MS, and is normalized to the sample with the highest level of each compound.

to papaverine (i.e. aromatic ring hydroxylation, four *O*-methylations and dehydrogenation), the bona fide participation of enzymes characterized *in vitro*, the sequence of reactions, and, in particular, the *N*-methylation status of the major pathway intermediates remains controversial (Pienkny *et al.*, 2009; Han *et al.*, 2010). In contrast to a previous model (Stadler and Zenk, 1990; Han *et al.*, 2010), our results suggest that papaverine biosynthesis does not primarily proceed through the *N*-methylated branch-point intermediate (*S*)-reticuline, which is involved in the formation of several BIA structural sub-groups (Ziegler and Facchini, 2008). Instead, the pathways leading to papaverine and *N*-methylated BIAs (e.g. noscapine and morphine) appear to bifurcate at (*S*)-coclaurine as a key branch-point intermediate (Figures 1 and S1). We also establish a role for known enzymes that perform 3′-hydroxylation (NMCH), *O*-methylation (6OMT, 4′OMT2, 7OMT and N7OMT), and *N*-methylation (CNMT) in the metabolic network responsible for the differential substitution of myriad BIAs.

6-*O*-methylation is the first step in the functionalization of (*S*)-norcoclaurine

Suppression of *6OMT* expression decreased total alkaloid levels by 73%, which was similar to the effect of reducing *NCS* transcripts (Lee and Facchini, 2010), suggesting a related regulatory function. NCS catalyzes the Pictet–Spengler condensation of dopamine and 4-hydroxyphenylacetaldehyde to yield the central intermediate (*S*)-norcoclaurine. Suppression of *6OMT* did not significantly affect *4′OMT1* or *4′*OMT2 transcript levels (Figure S4). *4′OMT2 has been shown to catalyze formation of* (*S*)-reticuline from (*S*)-3′hydroxy-*N*-methylcoclaurine (Figure 1), whereas no function for 4′OMT1 has been determined (Facchini and Park, 2003; Ziegler *et al.*, 2005). The strong effect of silencing *6OMT* on alkaloid content indicates that related *O*-methyltransferases in opium poppy do not exhibit sufficient 6-*O*-methylation activity to compensate for the silencing of *6OMT*. In contrast, *Eschscholzia californica* 4′OMT was shown to catalyze both *O*-methylation at C4′ and C6 on

various BIA substrates (Inui *et al.*, 2007). Although a single bi-functional *O*-methyltransferase was proposed, an uncharacterized 6OMT ortholog has also been reported in *E. californica* (Carlson *et al.*, 2006). 4′OMT2 from opium poppy has been reported to require a 3′-hydroxyl moiety and cannot accept (*S*)-norcoclaurine (Ziegler *et al.*, 2005). The role of 6OMT as a unique enzyme catalyzing a rate-limiting step in BIA biosynthesis that immediately follows formation of (*S*)-norcoclaurine is supported by efforts to engineer the pathway in microorganisms (Hawkins and Smolke, 2008; Minami *et al.*, 2008). In these studies, CNMT and 4′OMT were ineffective at forming substituted BIAs without inclusion of 6OMT. Expression of *Coptis japonica 6OMT* in cultured *E. californica* cells resulted in sevenfold higher alkaloid accumulation, but expression of *C. japonica 4′OMT* had no effect (Inui *et al.*, 2007). Coclaurine levels were unchanged despite the elevated 6OMT levels, suggesting that downstream enzymes are able to support increased flux through the BIA pathway. As VIGS is a gene knockdown rather than gene knockout technology, suppression of *6OMT* substantially reduced but did not prevent alkaloid production. Nevertheless, the reduced flux produced substantial differences in alkaloid profile compared with controls (Figure 6). The levels of all major products and most pathway intermediates were reduced, although some compounds were affected more than others.

Papaverine biosynthesis in opium poppy

The systematic suppression of six biosynthetic genes involved in two proposed biosynthetic routes to papaverine in opium poppy does not support a major role for (*S*)-reticuline as a pathway intermediate as recently suggested (Han *et al.*, 2010). The strong inverse correlation between *CNMT* transcript levels and papaverine accumulation shows that diversion of BIA metabolism away from *N*-methylated compounds, including (*S*)-reticuline, re-directs flux in favor of *N*-desmethylated alkaloids including papaverine and other 3′-hydroxylated and *O*-substituted derivatives of coclaurine and 4′-*O*-methylcoclaurine (Figures 4–6). In contrast, levels of reticuline and several *N*-methylated derivatives were reduced (Figure 6). The reduced phthalideisoquinoline and protoberberine alkaloid content in *CNMT*-suppressed plants (Figure 6) supports a role for (*S*)-reticuline as a key intermediate in formation of these BIA structural sub-groups. Interestingly, although the relative proportions of the morphinan alkaloid intermediates thebaine, oripavine and codeine were also lower, accumulation of morphine was unaffected by the reduced *CNMT* transcript level. (*S*)-Coclaurine clearly serves as a branch-point intermediate in the biosynthesis of *N*-desmethylated alkaloids such as papaverine and *N*-methylated compounds. The involvement of (*S*)-reticuline as an intermediate in papaverine biosynthesis was based on the relatively weak incorporation of labeled precursors (Han *et al.*, 2010). Interestingly, (*S*)-coclaurine was incorporated more effectively than (*S*)-reticuline, in support of the NH_3 pathway involving *N*-desmethylated compounds.

Additional evidence supports a role for (*S*)-coclaurine rather than (*S*)-reticuline as a key branch-point intermediate in papaverine biosynthesis. NMCH and 7OMT are required for the 3′-hydroxylation and 7-*O*-methylation of *N*-methylated intermediates leading to laudanosine, which subsequently requires *N*-demethylation in the NCH_3 pathway (Figures 1 and S1). NMCH and 7OMT are specific for the *N*-methylated substrates (*S*)-*N*-methylcoclaurine (Pauli and Kutchan, 1998) and (*R,S*)-reticuline (Ounaroon *et al.*, 2003), respectively, indicating that these enzymes can only operate in the putative NCH_3 pathway. However, suppression of *NMCH* and *7OMT* had no effect on papaverine accumulation (Figures 5 and 6). The significant increase in morphine accumulation resulting from reduced *7OMT* transcript levels may be explained by diversion of (*S*)-reticuline, via 7-*O*-methylation, away from the morphinan alkaloid pathway. In contrast, a reduced *N7OMT* transcript level correlated with a decrease in papaverine content (Figures 4 and 5). N7OMT catalyzes the 7-*O*-methylation of norreticuline, but not reticuline (Pienkny *et al.*, 2009), in support of a papaverine biosynthetic pathway involving *N*-desmethylated intermediates.

Suppression of *NMCH* had a marginal effect on total alkaloid accumulation, with thebaine and codeine showing the most pronounced reduction (Figure 4). However, the relative proportion of morphine, noscapine and papaverine was not significantly affected. A requirement for 3′-hydroxylation in papaverine biosynthesis, coupled with the substrate specificity of NMCH for (*S*)-*N*-methylcoclaurine (Pauli and Kutchan, 1998), suggests the occurrence of a similar enzyme that is uniquely able to 3′-hydroxylate (*S*)-coclaurine. Although uncharacterized, a homolog displaying 82% amino acid identity with NMCH has been detected in opium poppy (Desgagné-Penix *et al.*, 2012). Interestingly, *N*-methylation of *N*-desmethylated intermediates formed downstream of (*S*)-6-*O*-methylnorlaudanosoline (the 3′-hydroxyl derivative of coclaurine) provides a potential route to (*S*)-reticuline via 4′-*O*-methylation and *N*-methylation (Figure 8). An alternative route may be responsible for the limited effect of silencing *NMCH* on the levels of alkaloids, such as noscapine, derived from (*S*)-reticuline. However, as a gene knockdown technology, VIGS may only suppress certain transcripts to a level that remains above the threshold required to cause a phenotypic effect.

In related work, over-expression of *NMCH* increased the total alkaloid content of transgenic opium poppy plants by 450% without significantly altering individual alkaloid ratios, whereas antisense-mediated suppression of *NMCH* reduced total alkaloid accumulation by 84% (Frick *et al.*, 2007). Morphine, codeine and laudanine/laudanosine levels increased in antisense *NMCH* plants, but the relative

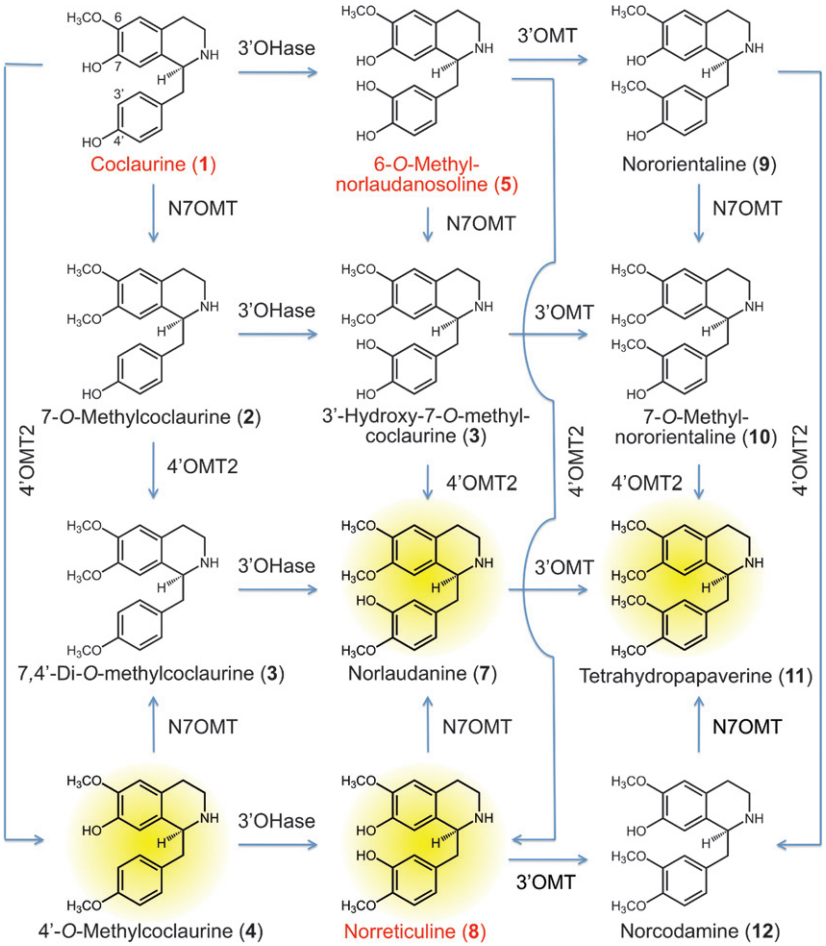

Figure 8. Putative BIA biosynthetic network for *N*-desmethylated compounds.
Previous work has shown that compounds in red are accepted as substrates by CNMT. Compounds highlighted in yellow were detected in opium poppy plants subjected to VIGS. The relative abundance of each compound is shown in Figure 7.

proportion of thebaine and oripavine decreased. Up- and down-regulation of other BIA biosynthetic genes was also attributed to over-expression and silencing, respectively, of *NMCH* (Frick *et al.*, 2007). In our experiments, only suppression of *CNMT* affected the transcript levels of other BIA biosynthetic genes (Figure S4), suggesting that the altered gene expression associated with the perturbation in *NMCH* transcript levels (Frick *et al.*, 2007) resulted from unrelated factors. NMCH has been proposed as a key step in BIA metabolism (Frick *et al.*, 2007), but our results do not support a role in papaverine biosynthesis (Figures 5 and 6).

Suppression of *4′OMT2* reduced total alkaloid content, although not as extensively as suppression of *6OMT*. Also, similar to the suppression of *6OMT* and in contrast to *NMCH*, all major alkaloids including papaverine were affected (Figure 6). Our VIGS results support a role for 4′OMT2 in formation of both *N*-methylated and *N*-desmethylated intermediates (Figures 8 and S7). 4′OMT2 from opium poppy has been reported not to accept coclaurine or *N*-methylcoclaurine as substrates owing to a purported requirement for a 3′-hydroxyl moiety (Frenzel and Zenk, 1990; Ziegler *et al.*, 2005). However, 4′OMT2 does not appear to exclude substrates based on their *N*-methylation status. The suggestion that (*S*)-reticuline is a key intermediate in papaverine biosynthesis was based largely on the feeding of labeled (*S*)-reticuline to opium poppy seedlings (Han *et al.*, 2010). Most of the labeled (*S*)-reticuline was transformed into thebaine, with relatively low incorporation into laudanine, laudanosine, tetrahydropapaverine and papaverine. However, the more efficient incorporation of laudanine and laudanosine into papaverine prompted the conclusion that papaverine is derived from *N*-methylated compounds. Although our VIGS results are at variance with this conclusion, a minor *N*-methylated pathway to papaverine is possible.

Biosynthetic networks in BIA metabolism

Some enzymes in specialized metabolism, including many methyltransferases, are not stereospecific and exhibit a relatively broad substrate range. For example, 6OMT from opium poppy and *C. japonica* has been shown to accept (*S*) and (*R*) epimers of norcoclaurine, norlaudanosoline and its *N*-methylated derivative laudanosoline (Sato *et al.*, 1994; Morishige *et al.*, 2000; Ounaroon *et al.*, 2003). Similarly,

CNMT catalyzed the *N*-methylation of all tested *N*-desmethylated BIAs, including coclaurine, norreticuline and 6-*O*-methylnorlaudanosoline (Choi *et al.*, 2001, 2002). The promiscuity of these enzymes with respect to related BIA substrates suggests that the established linear biosynthetic scheme from (*S*)-norcoclaurine to (*S*)-reticuline is an over-simplification of a more complex phenomenon. Our results show that certain BIA biosynthetic enzymes function in multi-dimensional metabolic grids involving a prescribed set of several intermediates, some of which proceed to various branch pathways. For example, 4′OMT2 and N7OMT may each operate at six points in a hypothetical arrangement of intermediates between (*S*)-coclaurine and (*S*)-tetrahydropapaverine (Figure 8). An as yet undiscovered 3′-hydroxylase and 3′-*O*-methyltransferase enzymes may each catalyze four potential conversions. In a coordinate metabolic grid representing all possible routes between (*S*)-*N*-methylcoclaurine and (*S*)-laudanosine, 4′OMT2 and 7OMT would each be responsible for six possible steps, whereas NMCH and an undiscovered 3′-*O*-methyltransferase are implicated in four hypothetical reactions (Figure S7). Interestingly, the primary endpoint for *N*-desmethylated BIA metabolism is the tetra-*O*-methylated tetrahydropapaverine, which is dehydrogenated to papaverine. In contrast, flux toward the corresponding *N*-methylated compound laudanosine is minimal compared with (*S*)-reticuline, which lacks *O*-methyl groups at C7 and C3′. The perturbation of hitherto accepted pathways and the revelation of alternative routes have been reported in engineered plants and microbes. For example, silencing of *BBE* in cultured *E. californica* cells resulted in reduced sanguinarine levels and accumulation of reticuline, 1,2-dehydroreticuline and laudanine, which are normally minor alkaloids (Fujii *et al.*, 2007).

The two schemes in Figures 8 and S7 are connected at each node by the potential *N*-methylation of intermediates via CNMT. The occurrence of corresponding *N*-desmethylated and *N*-methylated BIAs is suggestive of the potential substrate preference of CNMT. For example, the characterized CNMT substrate coclaurine (Choi *et al.*, 2002) was not detected (Figure 8), but its *N*-methylated derivative *N*-methylcoclaurine occurred in all plant lines (Figures 6 and S7). The reduced *N*-methylcoclaurine level in *CNMT*-suppressed plants is in agreement with the corresponding enzyme function determined *in vitro*. 4′-*O*-methyl-*N*-methylcoclaurine and laudanine levels were also reduced in *CNMT*-suppressed plants (Figure 6), suggesting that 4′-*O*-methylcoclaurine and norlaudanine, respectively, are also CNMT substrates (Figure 8).

Norlaudanosoline and laudanosoline were reported as effective substrates for 6-*O*-methylation by *C. japonica* 4′OMT, but 4′-*O*-methylation only occurred efficiently for laudanosoline due to a suggested requirement for *N*-methylation by CNMT (Morishige *et al.*, 2000). The detection of 4′-*O*-methylcoclaurine, norreticuline, norlaudanine and tetrahydropapaverine shows that 4′-*O*-methylation can occur prior to *N*-methylation in opium poppy, indicating that the substrate specificity of CNMT (and even certain *O*-methyltransferases), and thus the sequence of reactions, are species-specific. Norlaudanine was only detected in *CNMT*-suppressed plants (Table S2), whereas norcodamine was not (Figures 6 and 7 and Table S2). However, levels of palaudine and pacodine, the respective dehydrogenated derivatives of each compound (Figure S9), were elevated in *CNMT*-suppressed plants (Figures 6 and 7). Pacodine accumulation also increased in *N7OMT*-suppressed plants, whereas codamine levels were higher in *7OMT*-suppressed plants compared with controls. *N*-Desmethylated compounds occurred at significantly lower levels than their *N*-methylated analogs, and 7-*O*-methylated compounds were generally more abundant than those with 3′-*O*-methyl groups (Table S2).

In conclusion, using virus-induced gene silencing in one variety of opium poppy, we have shown that the major pathway to papaverine involves *N*-desmethylated intermediates and does not primarily proceed via (*S*)-reticuline. Early BIA metabolism flows through a metabolic grid composed of differentially substrate- and/or regio-specific 3′-hydroxylases, *O*- and *N*-methyltransferases and dehydrogenases. Major routes to branch-point intermediates converted to the main alkaloids in opium poppy latex (e.g. papaverine, noscapine and morphine) may be perturbed through suppression of individual biosynthetic genes.

EXPERIMENTAL PROCEDURES

Plant materials

Seeds of opium poppy (*Papaver somniferum* L. cultivar Bea's Choice) (Basement Shaman, http://www.basementshaman.com) were sown on a soil mixture consisting of baked clay medium and peat (1:2), and plants were cultivated at 20°C/15°C (light/dark) under 500 W metal halide lights (at a density of one light per 5 m^2 and a distance of 1 m from the soil surface) with a photoperiod of 16 h. Plants were fertilized weekly using water-soluble 20-20-20 NPK fertilizer with a concentration of approximately 200 ppm nitrogen.

Chemicals

Morphine and codeine were gifts from Sanofi-Aventis (http://en.sanofi-aventis.com). (*R,S*)-Tetrahydropalmatine, (*R,S*)-stylopine, (*R,S*)-canadine, (*S*)-scoulerine, (+/−)-pavine, thebaine and oripavine were obtained as described previously (Liscombe and Facchini, 2007; Hagel and Facchini, 2010). Tetrahydropapaverine was isolated as a contaminant of commercial (+/−)-pavine. Narcotoline was isolated from the opium poppy cultivar Marianne using methods described previously for the isolation of thebaine and oripavine (Hagel and Facchini, 2010). Dihydrosanguinarine was prepared by $NaBH_4$ reduction (Schumacher and Zenk, 1988). (*S*)-Reticuline was a gift from Tasmanian Alkaloids Pty Ltd (http://www.tasalk.com). Sanguinarine, papaverine, noscapine and dextromethorphan were purchased from Sigma-Aldrich (http://www.sigmaaldrich.com).

Vector construction

Unique regions of target gene cDNAs (Figure S2) were amplified by PCR using specific primer pairs (Table S1). Flanking *Bam*HI (or *Xba*I) and *Xho*I restriction endonuclease sites were added to primers as indicated. PCR products were ligated into pTRV2 (Liu *et al.*, 2002), and the constructs were sequenced to confirm correct assembly. The empty pTRV2 vector, the various pTRV2 constructs and pTRV1 (Liu *et al.*, 2002) were independently mobilized in *A. tumefaciens* strain GV3101.

VIGS

Agrobacterium tumefaciens strains harboring pTRV1 and various pTRV2 vectors were cultured in 500 ml LB medium supplemented with 10 mM MES, pH 6.0, 20 μM acetosyringone and 50 μg ml^{-1} kanamycin sulfate. Cultures were grown for 24 h at 28°C on a gyratory shaker at 180 rpm, and bacteria were harvested by centrifugation at 3000 ***g*** for 20 min and resuspended in infiltration buffer (10 mM MES, pH 6.0, 200 μM acetosyringone and 10 μM $MgCl_2$) to an optical density of 2.5 at 600 nm. Cultures harboring the various pTRV2 constructs were mixed at a ratio of 1:1 v/v with cultures containing pTRV1, and incubated at 25°C for 3 h prior to infiltration. Opium poppy seedlings were independently infiltrated at the two-leaf stage (approximately 18–21 days) using a 1 ml syringe, and plants were cultivated for 45–60 days. Plant tissues for gene expression (stems) and alkaloid (latex) analyses were harvested from immediately below the first flower buds 1–2 days before anthesis and stored at -80°C until analysis. VIGS efficiency was determined by suppression of the opium poppy phytoene desaturase gene as described previously (Hagel and Facchini, 2010), and was typically 15-20% based on the percentage of plants that showed photobleaching.

cDNA synthesis

Stem segments (approximately 1 cm) harvested from below the flower buds of opium poppy plants infiltrated with *A. tumefaciens* harboring TRV1 and various TRV2 constructs were ground to a fine powder under liquid nitrogen and total RNA was isolated as described previously (Desgagné-Penix *et al.*, 2010). First-strand cDNA was synthesized for 50 min at 37°C from 1 μg total RNA using Moloney murine leukemia virus reverse transcriptase (Invitrogen, http://www.invitrogen.com) in 20 μl reactions containing 2.5 mM oligo$(dT)_{20}$VN primers, buffer (250 mM Tris/Cl, pH 8.3, 375 mM KCl, 15 mM $MgCl_2$), 0.1 M DTT, dNTPs (0.5 mM each) and 2 units RNase OUT ribonuclease inhibitor (Invitrogen). The reaction was stopped by incubation at 70°C for 15 min. The synthesis of cDNA and the presence of the TRV coat protein transcripts were confirmed by PCR using specific GAPDH and TRV primers (Table S1) as described previously (Martin-Hernandez and Baulcombe, 2008).

Real-time quantitative PCR

Real-time quantitative PCR was performed on triplicate technical replicates of triplicate biological samples from each of nine plants confirmed to contain TRV coat protein transcripts (Figure S2). PCR mixtures included 1 × Power SYBR Green PCR Master Mix (Applied Biosystems, http://www.appliedbiosystems.com), forward and reverse primers (300 nM each; Table S1) and 1 μl of the cDNA synthesis reaction. Real-time quantitative PCR specificity was evaluated by subjecting all amplicons to a melt-curve analysis using the dissociation method (Applied Biosystems). PCR conditions were 2 min at 50°C and 10 min at 95°C, followed by 40 cycles of denaturation (15 sec at 95°C) and annealing/extension (60 sec at 72°C). Fluorescence signal intensities were recorded on a ABI 7300 real-time PCR system and analyzed using SDS software (Applied Biosystems). The threshold (C_t) value for each targeted gene transcript was normalized against the C_t value for the housekeeping gene ubiquitin, which was used as the reference transcript (Lee and Facchini, 2011). Mean C_t values were calculated from technical triplicates, and the relative levels of transcript encoding each enzyme were compared between plants infiltrated with control (calibrator) and gene-specific pTRV2 constructs using the relative quantification $2^{-\Delta\Delta C_t}$ method (Livak and Schmittgen, 2001; Schmittgen and Livak, 2008).

TLC and HPLC

For TLC, latex samples were resuspended in 50 μl methanol, vortexed, incubated at room temperature for 30 min, and 10 μl were spotted on Silica Gel 60 F_{254} plates (EMD Chemicals, http://www.emdchemicals.com). Compounds were separated using acetone/toluene/NH_3 ethanol (45:45:10) as the solvent system, and visualized under 254 nm illumination. Major alkaloids were identified based on their migration distances relative to the solvent front (R_F values) compared with those of authentic standards. For HPLC, the latex protein concentration was determined (Bradford, 1976). Dextromethorphan (2 μg) was added as an internal standard to a volume of each aqueous latex extract containing 50 μg protein, and the samples were extracted in 100 μl methanol for 2 h in at room temperature. Extracts were centrifuged at 16 000 ***g*** for 10 min, the supernatants were transferred to a new tube and reduced to dryness, and the residues were resuspended in 100 μl methanol. Ten microliters were diluted in 100 μl of water/acetonitrile/phosphoric acid (98:1.96:0.04) and analyzed using a System Gold HPLC and photodiode array detector (Beckman-Coulter, http://www.beckmancoulter.com). Separations were performed at a flow rate of 1.5 ml min^{-1} on a LiChrospher RP-Select B 5 μm particle size column (150 mm length × 4.6 mm inside diameter) (Merck, http://www.merck.com), using a gradient of solvent A (water/acetonitrile/phosphoric acid 98:1.96:0.04) and solvent B (water/acetonitrile/phosphoric acid 1.96:98:0.04). Chromatography was initiated using a 9:1 ratio of solvent A to solvent B for 5 min. Subsequently, the gradient was increased to 65:35 ratio of solvent A to solvent B over 40 min, and then to 100% solvent B over 5 min. Alkaloids were monitored at 210 nm and identified based on their retention times and UV spectra compared with those of authentic standards. BIA levels are expressed as μg alkaloid per μg latex protein.

LC-MS

Opium poppy latex was collected in pre-weighed tubes and reduced to dryness. One milligram of dried latex was extracted in methanol (20 μl per mg). The extract was centrifuged for 10 min at 16 000 ***g***, and the supernatant was reduced to dryness in a new tube. The residue was resuspended in 500 μl methanol, diluted 1:10 in 10 mM ammonium acetate/acetonitrile (95:5), pH 5.5, and 10 μl was subjected to HPLC on a Zorbax SB C18 column (50 mm long × 2.1 mm inside diameter, 1.8 μm particle size; Agilent Technologies, http://www.agilent.com) using a gradient of 10 mM ammonium acetate/acetonitrile (95:5), pH 5.5 (solvent A) and acetonitrile (solvent B). The initial HPLC condition of 100% solvent A was changed linearly to a 1:1 ratio of solvent A to solvent B over 10 min, and then to a 1:99 ratio of solvent A to solvent B over 12 min. The mobile phase was maintained at a 1:99 ratio of solvent A to solvent B for 1 min, and was then returned to starting conditions at 13.1 min for a 4 min re-equilibration period. After HPLC, analytes were injected into an electrospray ionization source and detected using a 6410B triple-quadrupole mass analyzer (Agilent

Technologies) operating in positive ion mode (ESI^+-MS). The first two quadrupoles were set to ''radiofrequency only'' and the third quadrupole was scanned at a mass range of 100-600 *m/z* (MS2Scan function in the Agilent Mass Hunter software). Mass-to-charge (*m/z*) values for compounds in the latex extracts were used to design subsequent collision-induced dissociation (CID) experiments. Each *m/z* value was isolated in quadrupole 1 and subjected to CID in quadrupole 2 at the collision energies listed in Table S3. Multiple reaction monitoring (MRM) and ESI^+-MS/MS were used to determine the relative abundance of selected BIAs as described previously (Farrow *et al.*, 2012). Data are expressed relative to the total content of identified or annotated alkaloids in plants infiltrated with the pTRV2 control construct (Table S2).

Compound characterization

Compound characterization criteria (Table S3) were based on established metabolomics guidelines (Neuman and Böcker, 2010). Alkaloids with available authentic standards were identified based on LC retention times and positive-mode electrospray ionization collision-induced dissociation (ESI^+-CID) spectra. Several alkaloids were annotated based on a match between empirical ESI^+-CID and published reference spectra. Other compounds were characterized as either specific alkaloids or possessing a BIA backbone structure by inference based on fragment ions induced by ESI^+-CID as described below.

BIAs have been extensively investigated by LC-MS (Budzikiewicz *et al.*, 1964; Sariyar *et al.*, 1990; Fabre *et al.*, 2000; Gioacchini *et al.*, 2000; Raith *et al.*, 2003; Hirata *et al.*, 2004; Kotake *et al.*, 2004; Poeaknapo *et al.*, 2004; Stévigny *et al.*, 2004; Schmidt *et al.*, 2005, 2007; Wu and Huang, 2006; Gesell *et al.*, 2009), and characteristic ESI^+-CID fragmentation mechanisms have been described (Schmidt *et al.*, 2005, 2007). Several compounds were characterized as BIAs based on generation of certain fragment ions. Formation of an ion corresponding to loss of ammonia or methylamine indicated whether the compound was *N*-methylated or *N*-desmethylated, respectively (Figure S8). The benzylisoquinoline moiety is produced by rearrangement, with reversed charge distribution involving the proton on the tetraisoquinoline nitrogen and the aromatic ring of the benzyl substituent (Schmidt *et al.*, 2005). The complementary ion, representing the benzyl group, is formed by a secondary fragmentation event. In summary, fragmentation of BIAs produces the diagnostic ions $[M+H]^+$, $[M+H\text{-}NH_3$ or $M+H\text{-}NCH_3]^+$, [M+H isoquinoline]$^+$ and [M+H benzyl]$^+$ that are useful for characterization. Some, but not all, of the substitutions on the benzyl and isoquinoline moieties can be determined. As an example, the complete characterization of 4′-*O*-methylcoclaurine is described here. The $[M+H]^+$ of 300 is the same as for *N*-methylcoclaurine, but the retention time is different (Table S3). The $[M+H]^+$ for coclaurine is 14 mass units lower, corresponding to a methyl group. A diagnostic fragment ion $[M+H\text{-}NH_3]^+$ at 283 indicates that the compound is not *N*-methylated. The most intense fragment ion at 121 corresponds to the benzyl moiety [M+H benzyl]$^+$, with an additional 14 mass units compared with coclaurine or *N*-methylcoclaurine. The isoquinoline fragment [M+H isoquinoline]$^+$ at 175 is identical to that of coclaurine. Furthermore, alkaloids without a 3′-hydroxyl function, such as norcoclaurine, coclaurine and *N*-methylcoclaurine, typically show [M+H benzyl]$^+$ as the most intense fragment ion due to a reduced ability to stabilize the benzyl leaving group (Schmidt *et al.*, 2005, 2007). In contrast, compounds with a 3′-hydroxyl function, such as reticuline or norreticuline, show [M+H isoquinoline]$^+$ as the major fragment ion. A similar strategy was used to characterize other BIAs (Figure S8 and Table S3). Chemical structures for all identified, annotated and characterized compounds are shown in Figure S6.

Statistical analysis

Student's *t* test was used with the following parameters: arguments, array1 (pTRV2 control values) and array2 (one pTRV2-silenced set of values), two-tailed and paired test type. Significance was determined at $P < 0.05$ and $P < 0.01$.

ACKNOWLEDGEMENTS

We thank Savithramma Dinesh-Kumar (Department of Plant Biology, University of California at Davis, CA, USA) for providing the pTRV1 and pTRV2 plasmids. This work was funded by Discovery, Strategic Project, and Research Tools and Infrastructure grants from the Natural Sciences and Engineering Research Council of Canada to P.J.F., who also holds the Canada Research Chair in Plant Metabolic Processes Biotechnology.

SUPPORTING INFORMATION

Additional Supporting Information may be found in the online version of this article:

Figure S1. Proposed papaverine biosynthetic pathways.

Figure S2. Regions of cDNAs encoding selected BIA biosynthetic enzymes used to construct pTRV2 vectors for VIGS analysis.

Figure S3. Detection of TRV in nine individual opium poppy plants subjected to VIGS and used for real-time quantitative PCR, HPLC and LC-MS analyses.

Figure S4. Relative transcript abundance for off-target biosynthetic genes in opium poppy plants subjected to VIGS using the indicated constructs.

Figure S5. Thin-layer chromatography of latex extracts from opium poppy plants subjected to VIGS using the indicated constructs.

Figure S6. Chemical structures and corresponding ESI^+-generated *m/z* values of identified, annotated and characterized compounds.

Figure S7. Putative BIA biosynthetic network for *N*-methylated compounds.

Figure S8. Characterization of compounds detected in latex extracts from opium poppy plants subjected to VIGS analysis.

Figure S9. Proposed formation of palaudine and pacodine, the dehydrogenated derivatives of norlaudanine and norcodamine, respectively.

Table S1. Sequences of PCR primers used to assemble VIGS constructs, confirm TRV infection and perform real-time quantitative PCR analysis.

Table S2. Relative abundance of alkaloids identified or annotated by LC-MS in plants infiltrated with *A. tumefaciens* harboring pTRV1 and the indicated pTRV2 construct.

Table S3. Chromatographic and spectral data used for identification and relative quantification of benzylisoquinoline alkaloids by LC-MS.

Please note: As a service to our authors and readers, this journal provides supporting information supplied by the authors. Such materials are peer-reviewed and may be re-organized for online delivery, but are not copy-edited or typeset. Technical support issues arising from supporting information (other than missingfiles) should be addressed to the authors.

REFERENCES

Barry, J.M. (2007) Treating erectile dysfunction in renal transplant recipients. *Drugs*, **67**, 975–983.

Battersby, A.R. (1963) Tilden Lecture: the biosynthesis of alkaloids. *Proc. Chem. Soc.* 189–200.

Battersby, A.R. and Binks, R. (1960) Biosynthesis of morphine: formation of morphine from norlaudanosoline. *Proc. Chem. Soc.* 360–361.

Battersby, A.R., Binks, R., Francis, R.J., McCaldin, D.J. and Ramuz, H. (1964) Alkaloid biosynthesis. Part IV. 1-Benzylisoquinolines as precursors of thebaine, codeine, and morphine. *J. Chem. Soc.* 3600–3610.

Battersby, A.R., Foulkes, D.M. and Binks, R. (1965) Alkaloid biosynthesis. Part VIII. Use of optically active precursors for investigations of the biosynthesis of morphine alkaloids. *J. Chem. Soc.* 3323–3332.

Battersby, A.R. and Harper, B.J.T. (1962) Alkaloid biosynthesis. Part I. The biosynthesis of papaverine. *J. Chem. Soc.* 3526–3533.

Bella, A.J. and Brock, G.B. (2004) Intracavernous pharmacotherapy for erectile dysfunction. *Endocrine*, **23**, 149–155.

Boswell-Smith, V., Spina, D. and Page, C.P. (2006) Phosphodiesterase inhibitors. *Br. J. Pharmacol.* **147**, S252–S257.

Bradford, M.M. (1976) Rapid and sensitive method for the quantitation of microgram quantities of protein utilizing the principle of protein–dye binding. *Anal. Biochem.* **72**, 248–254.

Brisman, J.L., Eskridge, J.M. and Newell, D.W. (2006) Neurointerventional treatment of vasospasm. *Neurol. Res.* **28**, 769–776.

Brochmann-Hanssen, E., Fu, C.C., Leung, A.Y. and Zanati, G. (1971) Opium alkaloids. X. Biosynthesis of 1-benzylisoquinolines. *J. Pharm. Sci.* **60**, 1672–1676.

Brochmann-Hanssen, E., Chen, C.-H., Chen, C.R., Chiang, H.-C., Leung, A.Y. and McMurtrey, K. (1975) Opium alkaloids. XVI. The biosynthesis of 1-benzylisoquinolines in Papaver somniferum. Preferred and secondary pathways; stereochemical aspects. *J. Chem. Soc. Perkin Trans.* **1**, 1531–1537.

Brochmann-Hanssen, E., Chen, C.-Y. and Linn, E.E. (1980) Biosynthesis of unnatural papaverine derivatives in *Papaver somniferum*. *J. Nat. Prod.* **43**, 736–738.

Budzikiewicz, H., Djerassi, C. and Williams, D.H. (1964) *Structure Elucidation of Natural Products by Mass Spectrometry*. San Francisco, CA: Holden-Day Inc.

Carlson, J.E., Leebens-Mack, J.H., Wall, P.K. *et al.* (2006) EST database for early flower development in California poppy (*Eschscholzia californica* Cham., Papaveraceae) tags over 6,000 genes from a basal eudicot. *Plant Mol. Biol.* **62**, 351–369.

Choi, K.B., Morishige, T. and Sato, F. (2001) Purification and characterization of coclaurine *N*-methyltransferase from cultured *Coptis japonica* cells. *Phytochemistry*, **56**, 649–655.

Choi, K.B., Morihige, T., Shitan, N., Yazaki, K. and Sato, F. (2002) Molecular cloning and characterization of coclaurine *N*-methyltransferase from cultured cells of *Coptis japonica*. *J. Biol. Chem.* **277**, 830–835.

Damen, L., Bruijn, J., Verhagen, A.P., Berger, M.Y., Passchier, J. and Koes, B.W. (2006) Prophylactic treatment of migraine in children. Part 2. A systematic review of pharmacological trials. *Cephalagia*, **26**, 497–505.

Desgagné-Penix, I., Khan, M.F., Schriemer, D.C., Cram, D., Nowak, J. and Facchini, P.J. (2010) Integration of deep transcriptome and proteome analyses reveals the components of alkaloid metabolism in opium poppy cell cultures. *BMC Plant Biol.* **10**, 252.

Desgagné-Penix, I., Farrow, S.C., Cram, D., Nowak, J. and Facchini, P.J. (2012) Integration of deep transcript and targeted metabolite profiles for eight cultivars of opium poppy. *Plant Mol. Biol.* **79**, 295–313.

Desvaux, P. (2005) An overview of the management of erectile disorders. *Presse Med.* **34**, 5–7.

Fabre, N., Claparois, C., Richelme, S., Angelin, M.-L., Fourasté, I. and Moulis, C. (2000) Direct characterization of isoquinoline alkaloids in a crude plant extract by ion-pair liquid chromatography-electrospray ionization tandem mass spectrometry: example of *Eschscholzia californica*. *J. Chromatogr. A*, **904**, 35–46.

Facchini, P.J. and Park, S.U. (2003) Developmental and inducible accumulation of gene transcripts involved in alkaloid biosynthesis in opium poppy. *Phytochemistry*, **64**, 177–186.

Farrow, S.C., Hagel, J.M. and Facchini, P.J. (2012) Transcript and metabolite profiling in cell cultures of 18 plant species that produce benzylisoquinoline alkaloids. *Phytochemistry*, **77**, 79–88.

Frenzel, T. and Zenk, M.H. (1990) *S*-Adenosyl-L-methionine:3′-hydroxyl-*N*-methyl-(*S*)-coclaurine-4′-*O*-methyltransferase, a regio- and stereoselective enzyme of the (*S*)-reticuline pathway. *Phytochemistry*, **29**, 3505–3511.

Frick, S., Kramell, R. and Kutchan, T.M. (2007) Metabolic engineering with a morphine biosynthetic P450 in opium poppy surpasses breeding. *Metab. Eng.* **9**, 169–176.

Fujii, N., Inui, T., Iwasa, K., Morishige, T. and Sato, F. (2007) Knockdown of berberine bridge enzyme by RNAi accumulates (*S*)-reticuline and activates a silent pathway in cultured California poppy cells. *Transgenic Res.* **16**, 363–375.

George, G.M., Bauer, R., Blennow, A., Kossmann, J. and Lloyd, J.R. (2012) Virus-induced multiple gene silencing to study redundant metabolic pathways in plants: silencing the starch degradation pathway in *Nicotiana benthamiana*. *Biotechnol. J.* **7**, 884–890.

Gesell, A., Rolf, M., Ziegler, J., Díaz-Chávez, M.L., Huang, F.-C. and Kutchan, T.M. (2009) CYP719B1 is salutaridine synthase, the C–C phenol-coupling enzyme of morphine biosynthesis in opium poppy. *J. Biol. Chem.* **284**, 24432–24442.

Gioacchini, A.M., Czarnocki, Z., Arazny, Z., Munari, I. and Traldi, P. (2000) Electrospray ionization, accurate mass measurements and multistage mass spectrometry experiments in the characterization of stereoisomeric isoquinoline alkaloids. *Rapid Commun. Mass Spectrom.* **14**, 1592–1599.

Hagel, J.M. and Facchini, P.J. (2010) Dioxygenases catalyze the *O*-demethylation steps of morphine biosynthesis in opium poppy. *Nat. Chem. Biol.* **6**, 273–275.

Han, X., Lamshöft, M., Grobe, N., Ren, X., Fist, A.J., Kutchan, T.M., Spiteller, M. and Zenk, M.H. (2010) The biosynthesis of papaverine proceeds via (*S*)-reticuline. *Phytochemistry*, **71**, 1305–1312.

Hawkins, K.M. and Smolke, C.D. (2008) Production of benzylisoquinoline alkaloids in *Saccharomyces cerevisiae*. *Nat. Chem. Biol.* **4**, 564–573.

Hirata, K., Poeaknapo, C., Schmidt, J. and Zenk, M.H. (2004) 1,2-Dehydroreticuline synthase, the branch point enzyme opening the morphinan biosynthetic pathway. *Phytochemistry*, **65**, 1039–1046.

Inui, T., Tamura, K.-i., Fujii, N., Morishige, T. and Sato, F. (2007) Overexpression of *Coptis japonica* norcoclaurine 6-*O*-methyltransferase overcomes the rate-limiting step in benzylisoquinoline alkaloid biosynthesis in cultured *Eschscholzia californica*. *Plant Cell Physiol.* **48**, 252–262.

Kotake, Y., Okuda, K., Kamizono, M., Matsumoto, N., Tanahashi, T., Hara, H., Caparros-Lefebvre, D. and Ohta, S. (2004) Detection and determination of reticuline and *N*-methylcoclaurine in the *Annonaceae* family using liquid chromatography-tandem mass spectrometry. *J. Chromatogr. B*, **806**, 75–78.

Lee, E.J. and Facchini, P.J. (2010) Norcoclaurine synthase is a member of the pathogenesis-related 10/Bet v1 protein family. *Plant Cell*, **22**, 3489–3503.

Lee, E.J. and Facchini, P.J. (2011) Tyrosine aminotransferase contributes to benzylisoquinoline alkaloid biosynthesis in opium poppy. *Plant Physiol.* **157**, 1067–1078.

Liscombe, D.K. and Facchini, P.J. (2007) Molecular cloning and characterization of tetrahydroprotoberberine *cis*-*N*-methyltransferase, an enzyme involved in alkaloid biosynthesis in opium poppy. *J. Biol. Chem.* **282**, 14741–14751.

Liscombe, D.K. and O'Connor, S.E. (2011) A virus-induced gene silencing approach to understanding alkaloid metabolism in *Catharanthus roseus*. *Phytochemistry*, **72**, 1969–1977.

Liu, Y., Schiff, M. and Dinesh-Kumar, S.P. (2002) Virus-induced gene silencing in tomato. *Plant J.* **31**, 777–786.

Livak, K.J. and Schmittgen, T.D. (2001) Analysis of relative gene expression data using real-time quantitative PCR and the $2^{-\Delta\Delta Ct}$ method. *Methods*, **25**, 402–408.

Martin-Hernandez, A.M. and Baulcombe, D.C. (2008) Tobacco rattle virus 16-kilodalton protein encodes a suppressor of RNA silencing that allows transient viral entry in meristems. *J. Virol.* **82**, 4064–4071.

McGeoch, R.J. and Oldroyd, K.G. (2008) Pharmacological options for inducing maximal hyperaemia during studies of coronary physiology. *Catheter. Cardiovasc. Interv.* **71**, 198–204.

Menniti, F.S., Chappie, T.A., Humphrey, J.M. and Schmidt, C.J. (2007) Phosphoesterase 10A inhibitors: a novel approach to the treatment of the symptoms of schizophrenia. *Curr. Opin. Investig. Drugs*, **8**, 54–59.

Minami, H., Kim, J.-S., Ikezawa, N., Takemura, T., Katayama, T., Kumagai, H. and Sato, F. (2008) Microbial production of plant benzylisoquinoline alkaloids. *Proc. Natl Acad. Sci. USA*, **105**, 7393–7398.

Mindea, S.A., Yang, B.P., Bendok, B.R., Miller, J.W. and Bather, H.H. (2006) Endovascular treatment strategies for cerebral vasospasm. *Neurosurg. Focus*, **21**, E13.

Morishige, T., Tsujita, T., Yamada, Y. and Sato, F. (2000) Molecular characterization of the *S*-adenosyl-L-methionine:3′-hydroxy-*N*-methylcoclaurine 4′-*O*-methyltransferase involved in isoquinoline alkaloid biosynthesis in *Coptis japonica*. *J. Biol. Chem.* **275**, 23398–23405.

Neuman, S. and Böcker, S. (2010) Computional mass spectrometry for metabolomics: identification of metabolites and small molecules. *Anal. Bioanal. Chem.* **398**, 2779–2788.

Ounaroon, A., Decker, G., Schmidt, J., Lottspeich, F. and Kutchan, T.M. (2003) (*R,S*)-Reticuline 7-*O*-methyltransferase and (*R,S*)-norcoclaurine 6-*O*-meth-

yltransferase of *Papaver somniferum* – cDNA cloning and characterization of methyl transfer enzymes of alkaloid biosynthesis in opium poppy. *Plant J.* **36**, 808–819.

Pauli, H.H. and Kutchan, T.M. (1998) Molecular cloning and functional heterologous expression of two alleles encoding (*S*)-*N*-methylcoclaurine 3′-hydroxylase (CYP80b1), a new methyl jasmonate-inducible cytochrome P-450-dependent monooxygenase of benzylisoquinoline alkaloid biosynthesis. *Plant J.* **13**, 793–801.

Pienkny, S., Brandt, W., Schmidt, J., Kramell, R. and Ziegler, J. (2009) Functional characterization of a novel benzylisoquinoline-*O*-methyltransferase suggests its involvement in papaverine biosynthesis in opium poppy (*Papaver somniferum* L.). *Plant J.* **60**, 56–67.

Poeaknapo, C., Fisinger, U., Zenk, M.H. and Schmidt, J. (2004) Evaluation of the mass spectrometric fragmentation of codeine and morphine after ^{13}C-isotope biosynthetic labeling. *Phytochemistry*, **65**, 1413–1420.

Priebe, H.J. (2007) Aneurysmal subarachnoid haemorrhage and the anaesthetist. *Br. J. Anaesth.* **99**, 102–118.

Raith, K., Neubert, R., Poeaknapo, C., Boettcher, C., Zenk, M.H. and Schmidt, J. (2003) Electrospray tandem mass spectrometric investigations of morphinans. *J. Am. Soc. Mass Spectrom.* **14**, 1262–1269.

Samanani, N., Liscombe, D.K. and Facchini, P.J. (2004) Molecular cloning and characterization of norcoclaurine synthase, an enzyme catalyzing the first committed step in benzylisoquinoline alkaloid biosynthesis. *Plant J.* **40**, 302–313.

Sariyar, G., Sari, A., Freyer, A.J., Guinaudeau, H. and Shamma, M. (1990) Quaternary isoquinoline alkaloids from *Papaver* species. *J. Nat. Prod.* **53**, 1302–1306.

Sato, F., Tsujita, T., Katagiri, Y., Yoshida, S. and Yamada, Y. (1994) Purification and characterization of *S*-adenosyl-L-methionine:norcoclaurine 6-*O*-methyltransferase from cultured *Coptis japonica* cells. *Eur. J. Biochem.* **225**, 125–131.

Schmidt, J., Raith, K., Boettcher, C. and Zenk, M.H. (2005) Analysis of benzylisoquinoline-type alkaloids by electrospray tandem mass spectrometry and atmospheric pressure photoionization. *Eur. J. Mass Spectrom.* **11**, 325–333.

Schmidt, J., Boettcher, C., Kuhnt, C., Kutchan, T.M. and Zenk, M.H. (2007) Poppy alkaloid profiling by electrospray tandem mass spectrometry and electrospray FT-ICR mass spectrometry after [*ring*-$^{13}C_6$]-tyramine feeding. *Phytochemistry*, **68**, 189–202.

Schmittgen, T.D. and Livak, K.J. (2008) Analyzing real-time PCR data by the comparative C_T method. *Nat. Protoc.* **3**, 1101–1108.

Schumacher, H.-M. and Zenk, M.H. (1988) Partial purification and characterization of dihydrobenzophenanthridine oxidase from *Eschscholtzia californica* cell suspension cultures. *Plant Cell Rep.* **7**, 43–46.

Srivastava, V.K., Agrawal, S. and Sahu, S. (2011) Association of acute onset hypertension and tachycardia following intracisternal papaverine administration during intracranial aneurysm surgery: a case report and review of the literature. *J. Clin. Anesth.* **23**, 224–226.

Stadler, R. and Zenk, M.H. (1990) A revision of the generally accepted pathway for the biosynthesis of the benzyltetrahydroisoquinoline reticuline. *Liebigs Ann. Chem.* **1990**, 555–562.

Stadler, R., Kutchan, T.M., Loeffler, S., Nagakura, N., Cassels, B. and Zenk, M.H. (1987) Revision of the early steps of reticuline biosynthesis. *Tetrahedron Lett.* **28**, 1251–1254.

Stévigny, C., Habib Jiwan, J.-L., Rozenberg, R., de Hoffman, E. and Quentin-Leclercq, J. (2004) Key fragmentation patterns of aporphine alkaloids by electrospray ionization multistage mass spectrometry. *Rapid Commun. Mass Spectrom.* **268**, 523–528.

Uprety, H., Bhakuni, D.S. and Kapil, R.S. (1975) Biosynthesis of papaverine. *Phytochemistry*, **14**, 1535–1537.

Wijekoon, C.P. and Facchini, P.J. (2012) Systematic knockdown of morphine pathway enzymes in opium poppy using virus-induced gene silencing. *Plant J.* **69**, 1052–1063.

Winterstein, E. and Trier, G. (1910) *Die Alkaloide.* Berlin: Verlag Gebrüder Bornträger.

Wu, W.N. and Huang, C.-H. (2006) Structural elucidation of isoquinoline, benzylisoquinoline, aporphine, and phenanthridine alkaloids using API-ionspray tandem mass spectrometry. *Chin. Pharm. J.* **58**, 41–55.

Ziegler, J. and Facchini, P.J. (2008) Alkaloid biosynthesis: metabolism and trafficking. *Annu. Rev. Plant Biol.* **59**, 735–769.

Ziegler, J., Diaz-Chavez, M.L., Kramell, R., Ammer, C. and Kutchan, T.M. (2005) Comparative macroarray analysis of morphine containing *Papaver somniferum* and eight morphine free *Papaver* species identifies an *O*-methyltransferase involved in benzylisoquinoline biosynthesis. *Planta*, **222**, 458–471.